Optimal Design of a Subsurface Redox Barrier

Ashok Chilakapati
Pacific Northwest National Laboratory, Richland, WA 99352

Harmful contaminants such as chromium (Cr^{+6}), and TCE can be removed from groundwater by reactions with reduced subsurface sediments. Establishing an in situ Fe(II) barrier through the reduction of soil-bound Fe(III) to Fe(II) by injecting a sodium dithionite ($Na_2S_2O_4$) solution is studied. Critical to this problem is the possible formation and expansion of a zone around the injection, where all the soil-bound Fe(III) is reduced to Fe(II). Different reaction models apply inside and outside of this zone so that a determination of this moving boundary is a fundamental part of the solution. The complete analytic solution to this problem was used to develop optimal process parameters, such as injection rate and operational time, that maximize the radius of the Fe(III)-reduced zone when a given mass of sodium dithionite is injected at a well. When a large reduction [>63% of initially present Fe(III)] is desired, the results indicate that it is better to use a low flow rate to form a Fe(III)-free zone around the injection. The opposite is true for smaller reductions (<63%), so that a faster injection rate that avoids the formation of the Fe(III)-free zone yields a larger reduction zone.

Introduction

Permeable reactive barriers in the flow path of a groundwater plume can help sequester the dissolved contaminants. The reactive nature of the barrier is dictated by the anticipated chemistry with the aqueous-phase contaminants. For redox-sensitive groundwater contaminants, the barrier may be made more reducing (or oxidizing) than elsewhere in the aquifer if the ensuing reactions destroy the contaminant, change it to a less toxic form, or decrease its mobility. For example, chromate in groundwater may be precipitated or immobilized in a reducing environment (Sass and Rai, 1987; Anderson et al., 1994; Kent et al., 1994). Anderson et al. (1994) have shown that the presence of even a small amount of Fe(II) can effectively reduce aqueous chromate. The abundance of Fe(III) oxides in the subsurface offers an *in situ* source of electron acceptor that can be utilized to create a reductive Fe(II) barrier. Researchers have studied the reduction of soil-bound Fe(III) to Fe(II) through biotic (Lovely, 1993; Gorby et al., 1994) and abiotic means (Amonette et al., 1994; Williams et al., 1994; Fruchter et al., 1996; Istok et al., 1999). Dissimulatory Fe(III)-reducing bacteria (DIRB) are subsurface microorganisms that utilize Fe(III) oxides as electron acceptors under anoxic conditions (Lovely, 1993). Encouraging the growth of DIRB with a substrate such as lactate, an Fe(II) zone may be established. On the abiotic side, chemical reagents such as dithionite ion ($S_2O_4^{-2}$) have been used to reduce Fe(III) to Fe(II) (Amonette et al., 1994). Injection of sodium dithionite solution into the soil to establish a Fe(II) zone in the flow-path of a chromium plume has recently been tested at Hanford (Fruchter et al., 1996).

The process of establishing an *in situ* Fe(II) zone is the focus here rather than the performance of such a reductive zone in arresting the migration of redox-sensitive contaminants. Batch, column, and pilot field experiments, followed by detailed modeling and analysis such as presented by Friedly et al. (1995) (for chromium transport), are necessary for estimating the effectiveness of a reactive barrier for a given contaminant. The shape and dimensions of the required barrier depend on a number of factors which include: the anticipated chemistry between Fe(II) and the contaminant plume in question; the reductive capacity of the barrier (total available Fe(III) for reduction); contaminant concentration; and the speed of the plume. The Damköhler number associated with the speed of the contaminant transformation reaction and the speed of groundwater is important in determining the minimum residence time required to decrease the contaminant levels below some threshold value. Loss of Fe(II) zone can also occur if the migrating groundwater is oxic, or in shallow aquifers by oxygen diffusion from the surface. The total mass of the contaminant that needs to be removed from groundwater dictates the required useful lifetime of the barrier. In

this case, the barrier should have a minimum width that allows a satisfactory sequestration (or degradation) of the contaminant even if a part of the barrier upstream has been compromised.

An analysis that takes all these factors into account and develops the specifications for the geometry of the barrier is an essential precursor to the study presented here. It is assumed here that the shape and dimensions of the required barrier have been specified with the only remaining task being the creation of such a barrier. While the required geometry of the barrier is specific to the contamination, the process of realizing such a barrier is fairly independent, discounting any adverse interaction between the reducing agent and the contaminant. Given that assumption, this article analyzes the process model that creates the Fe(II) barrier and optimizes the relevant parameters for creating the largest possible area with the desired concentration of Fe(II).

The case of a single injection well is considered, and the optimal injection rate and the required operational time that will maximize the Fe(II) zone for a given mass of dithionite is found. The streamtube reaction model for the generation of Fe(II) zone is described. An analytic solution to this model is obtained, and this solution is scaled to obtain the solution for the propagation of Fe(III)-reduced zone when the flow field is due to a single injection well. This solution is used to determine the optimal injection rate and the required time of operation that maximize the reduced zone.

Reaction Model

Abiotic reduction of Fe(III) by the dithionite ion, which is a strong reductant in basic solutions, is considered. Amonette et al. (1994) have described the aqueous chemistry of the dithionite ion and the transfer of electrons to Fe(III) in the solid phase that forms Fe(II). A simplified model of this process consists of three primary reactions: (1) the fast dissociation of $S_2O_4^{-2}$ to yield two sulphoxyl radicals SO_2^-; (2) the reaction of SO_2^- with Fe(III) to yield Fe(II) (and sulfite or bisulfite); (3) the slow disproportionation of $S_2O_4^{-2}$ to yield thiosulfate or bisulfite.

Reaction 1 is fast and irreversible, so it may be combined with Reactions 2 and 3.

$$S_2O_4^{-2} + 2Fe^{+3} + 2H_2O \xrightarrow{k_1} 2SO_3^{-2} + 2Fe^{+2} + 4H^+ \quad \text{Redox} \quad (1)$$

$$2S_2O_4^{-2} + H_2O \xrightarrow{k_2} 2HSO_3^- + S_2O_3^{-2} \quad \text{Disproportionation} \quad (2)$$

Reaction 1 is the useful reaction that generates Fe(II), whereas Reaction 2 represents a sediment-catalyzed disproportionation of dithionite. Once Fe(II) is generated, a contaminant such as chromate is reduced by Fe(II), forming an insoluble complex, thus removing it from the groundwater

$$3Fe^{+2} + CrO_4^{-2} + 5H^+ \rightarrow Cr(OH)_3\downarrow + 3Fe^{+3} + H_2O$$

The two important processes in creating a subsurface Fe(II) barrier through dithionite injection are: (a) convection, which delivers dithionite from the injection well; (b) the redox and disproportionation reactions that generate Fe(II) and consume dithionite. The effect of diffusion is minor, because the primary mechanism that makes dithionite available in the field is convection. As for the reaction rates, Amonette et al. (1994) and Istok et al. (1999) have shown in their experiments with Hanford sediments that: (1) the rate of redox reaction may be approximated as $k_1\,[S_2O_4^{-2}]$ if Fe^{+3} is present and as zero in its absence; (2) the rate of disproportionation reaction is $k_2\,[S_2O_4^{-2}]$.

In the absence of diffusion, transport occurs along streamtubes connecting the upstream and downstream locations in the flow field. When the flow is steady, the spatial configuration of these connecting streamtubes is fixed, and the response at the downstream location for any input of solutes upstream can be computed as the solutes are delivered through these streamtubes. The concentrations of the solutes delivered downstream by a streamtube are obtained by solving a one-dimensional (1-D) convection-reaction problem along the streamtube. Reactive transport along a streamtube is conveniently described by the variables time t and travel-time τ to any distance along the streamtube, measured from the upstream location (Cvetkovic and Dagan, 1994). The utility of this formulation arises from the fact that the solution obtained in terms of the time t and travel-time τ is directly applicable to any other connecting streamtube when the initial conditions are identical. The streamtube solution can also be used in conjunction with any other flow field with the same underlying reaction problem and initial conditions. Thus, the solution to a number of multidimensional convection-reaction problems can be obtained by first solving the convection of the reaction system in a single streamtube (Chilakapati and Yabusaki, 1999). Using the notation C as the concentration of $S_2O_4^{-2}$ and S as the concentration of Fe^{+3}, the governing equations for the evolution of C, S in a 1-D streamtube are

$$\frac{\partial C}{\partial t} + \frac{\partial C}{\partial \tau} = -(k_1 + k_2)C, \quad \frac{\partial S}{\partial t} = -2k_1 C, \quad \text{when } S > 0 \quad (3)$$

$$\frac{\partial C}{\partial t} + \frac{\partial C}{\partial \tau} = -k_2 C, \quad \frac{\partial S}{\partial t} = 0, \quad \text{when } S = 0 \quad (4)$$

The uniform initial conditions on $\{C, S\}$ and the boundary condition on C are

$$\text{IC:} \quad C(0,\tau) = 0, S(0,\tau) = S_0, \quad \text{BC:} \quad C(0 < t < \Delta, 0) = C_i \quad (5)$$

The distribution of Fe(III) oxides in the field is rarely uniform. Lenticular-shaped iron-oxide inclusions (Reidel et al., 1994; Szecsody et al., 1988) are common as are those that are accessible through intragrain diffusion (Friedly et al., 1995). The available Fe(III) (S_0) in Eq. 5 is the iron oxide that is readily accessible to the surrounding fluid without including any Fe(III) that might only be accessible via intragrain diffusion. The use of uniform S_0 is still an approximation that makes the model mathematically tractable and allows us to solve the multidimensional reactive transport problem using the solution to the 1-D model (Eqs. 3 through 5). This is achieved by mapping spatial locations to the time τ it takes

to travel along a streamline originating at injection (Chilakapati and Yabusaki, 1999). These solutions are useful in many field situations where the detailed distribution of iron oxide is not available and in the verification of approximate numerical models.

Solution

Upon injection of dithionite, $S(t,\tau)$ will start to decrease from S_0 according to Eq. 3. Let $S(t,\tau)$ remain nonzero at all τ until a time $t_0^{\min} > 0$. The complete solution for $\tau < t < t_0^{\min}$ is then obtained by solving Eqs. 3 and 5

$$C(t,\tau) = C_i \exp\left[-(k_1 + k_2)\tau\right] \tag{6}$$

$$S(t,\tau) = S_0 - 2k_1(t-\tau)C_i \exp\left[-(k_1 + k_2)\tau\right] \tag{7}$$

If the duration of dithionite injection (pulse length Δ) is long enough, S will go to zero first at $\tau = 0$. This is because $S(t,\tau)$ in Eq. 7 is a minimum at $\tau = 0$. The time at which this happens defines $t_0^{\min}$. It is obtained by solving $S(t_0^{\min}, 0) = 0$ for $t_0^{\min}$ in Eq. 7

$$t_0^{\min} = S_0/(2k_1C_i) \tag{8}$$

If the injection continues for a long enough time, S could go to zero over a part of the τ-domain. When this happens, Eq. 3 applies over the part of the τ-domain where $S > 0$, and Eq. 4 applies elsewhere. For a finite pulse (of duration Δ) injection of dithionite, the nature of the problem alters again when the injection stops. The development of the solution is made clear by considering the propagation wave fronts in the $t-\tau$ plane. Figure 1 shows the expected wave fronts and how they divide the $t-\tau$ plane into different regions (region I through region V). The characteristics for dithionite are linear with unit slope, because dithionite moves unretarded with pore water. The leading edge of the dithionite front starts at the origin, and the trailing edge at time $t = \Delta$ when the pulse ends. Nonzero concentrations of dithionite are expected only in the region bound by these two waves.

Two cases may be discerned depending on whether an Fe(III)-free zone will form. First, consider the case where the injection is long enough so that an Fe(III)-free zone does form. This is shown in Figure 1B. S goes to zero first at $\tau = 0$ at time $t = t_0^{\min}$. Because the reduction reaction rate is finite, it is easily anticipated that the speed of propagation of the $S = 0$ front will be less than that of dithionite waves (this is proved more rigorously in later sections). Further, since the reduction rate is proportional to the concentration of dithionite, the speed of propagation of the $S = 0$ front continues to decrease as it expands deeper into the τ-domain. This is because the concentration of dithionite should decrease with increasing τ. When the trailing edge of dithionite pulse intersects the $S = 0$ front, the expansion stops because there is no more dithionite available for reducing S at the front. The simpler (but important for some field situations) second case, when the injection is not long enough to form an Fe(III)-free zone, is sketched in Figure 1A. In this case, the $t-\tau$ plane is divided into two regions I and I′.

The solution for dithionite concentration is obtained by following the characteristics in each of the five regions and

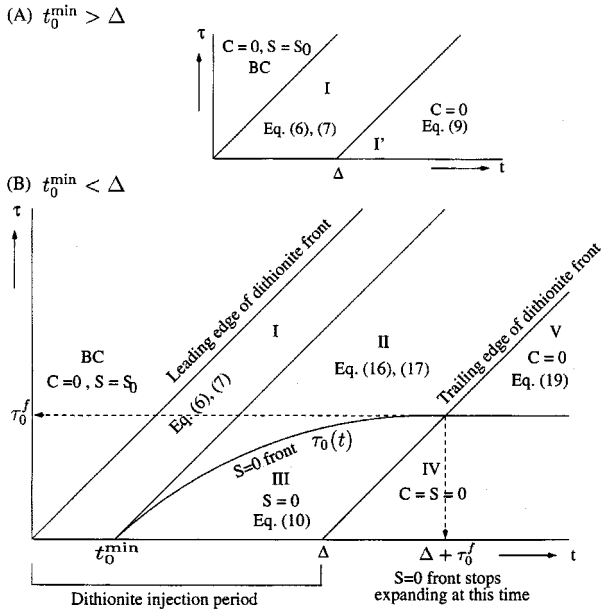

Figure 1. (A) Wave when the duration of injection $\Delta < t_0^{\min}$ ($S = 0$ front is not formed); (B) propagation of waves in the $t-\tau$ plane when $\Delta > t_0^{\min}$.

Dithionite waves propagate along unit-slope characteristics, whereas the propagation of the $S = 0$ front is slower and nonlinear.

applying the appropriate reaction model depending on the presence or absence of Fe(III). For example, the solution in region I is obtained by solving Eq. 3 alone, and the solution in region III is obtained by solving Eq. 4 alone. However, the solution at a point in region II requires the determination of the $S = 0$ front. This is because the unit-slope characteristic through that point intersects the $S = 0$ front. The dithionite concentration in region II is obtained by allowing reaction according to Eq. 4 for a portion of the time and according to Eq. 3 for the remainder, applicable in regions III and II, respectively. In what follows the different solution regions (I through V) that appear and disappear at various times are examined. Solutions are developed for the propagation of the $S = 0$ front and the complete solution to C and S in all five regions.

Regions I and I′

Region I is the $t-\tau$ region where S is always nonzero and $C = C_i$ is the boundary data along the t-axis. Equations 6 and 7 furnish the complete solution. S will not go to zero for any τ if the duration (Δ) of dithionite injection is less than $t_0^{\min}$. Region I′ in Figure 1A is formed in this case. $C \equiv 0$ in region I′ because injection stops at time $t = \Delta$. A location τ becomes a part of region I′ at the time $\tau + \Delta$ when the dithionite pulse passes by that location completely. The solution for S in region I′ is given by Eq. 7 with $t = \Delta + \tau$.

$$S(t,\tau) = S_0 - 2k_1\Delta C_i \exp\left[-(k_1 + k_2)\tau\right] \tag{9}$$

No reduction of S can take place in region I′ because the

dithionite pulse has completely passed this region. The solution for S in region I′ will not change with time.

Regions II and III

An Fe(III)-free zone will form if both Δ and t are greater than $t_0^{\min}$. S will first go to zero at $\tau = 0$ (when $t = t_0^{\min}$), and the $S = 0$ front marches into the τ-domain as time increases. Three features of the problem are critical to obtaining a solution in region II:

(1) The speed of propagation of $S = 0$ front can never be greater than unity, the speed of dithionite waves. The unit-slope characteristic originating at ($t = t_0^{\min}$, $\tau = 0$) will always be above the position $\tau_0(t)$ of the $S = 0$ front at any time t, as shown in Figure 1B. While this was anticipated on physical grounds in the drawing of Figure 1B, it is proved here. $\tau_0(t)$ and $t - t_0^{\min}$ are identically zero when $t = t_0^{\min}$ but expand outward at different rates as t increases beyond $t_0^{\min}$. The maximum rate of decrease of S at any τ occurs when C is maximum at that τ. The maximum possible value of C that arrives at any τ is $C_i \exp(-k_2\tau)$, which occurs when no redox reaction takes place between 0 and τ (that is, $S = 0$ between 0 and τ). At this maximum rate, S at that τ decreases according to

$$S(t,\tau) = S_0 - 2k_1(t-\tau)C_i \exp(-k_2\tau)$$

So the earliest S can go to zero at any τ is the time $\tau + t_0^{\min}\exp(k_2\tau)$. Thus, if at time t the front is at $\tau_0(t)$, then $t \geq \tau_0(t) + t_0^{\min}\exp[k_2\tau_0(t)]$ or

$$t - t_0^{\min} \geq \tau_0(t) + t_0^{\min}\exp\left[k_2\tau_0(t)\right] - t_0^{\min} \geq \tau_0(t)$$

proving that $\tau_0(t)$ is always less than $t - t_0^{\min}$.

(2) $\tau_0(t)$ propagates at less than unit speed, so dithionite waves originating in region III ($t_0^{\min} < t < \Delta$) will overtake the $S = 0$ front to reach region II. Dithionite reacts according to Eq. 4 in region III because $S = 0$. The solution in region III is

$$C(t,\tau) = C_i \exp(-k_2\tau), \quad S(t,\tau) = 0 \tag{10}$$

(3) Region II presents a moving boundary $\tau_0(t)$, whose position is not known ahead of time. The solution in region II, however, depends on the entire history of propagation of the $\tau_0(t)$ front from time $t_0^{\min}$ through t. This is because (a) the concentration of dithionite entering region II is $C_i \exp[-k_2\tau_0(t)]$, (b) the decrease in S at any τ in region II is a function of *all* the C that passes through that τ; and (c) the unknown function $\tau_0(t)$ itself must be obtained as the τ in region II where S goes to zero at time t. While the solution of Eqs. 3 or 4 is straightforward, the key issue here is not knowing the τ-range over which each of these equations is applicable at any time t. Thus, the first step is to determine $\tau_0(t)$. Using items (a) through (c) leads to an integral equation governing the propagation of $\tau_0(t)$. Solving for $\tau_0(t)$ then allows an appropriately combined solution of Eqs. 3 and 4 to yield C and S in region II.

Determination of $\tau_0(t)$. Figure 2A shows a location τ that will be a part of region II from time $t_0^{\min} + \tau$ until time t, when $\tau_0(t) = \tau$. All unit-slope characteristics passing through

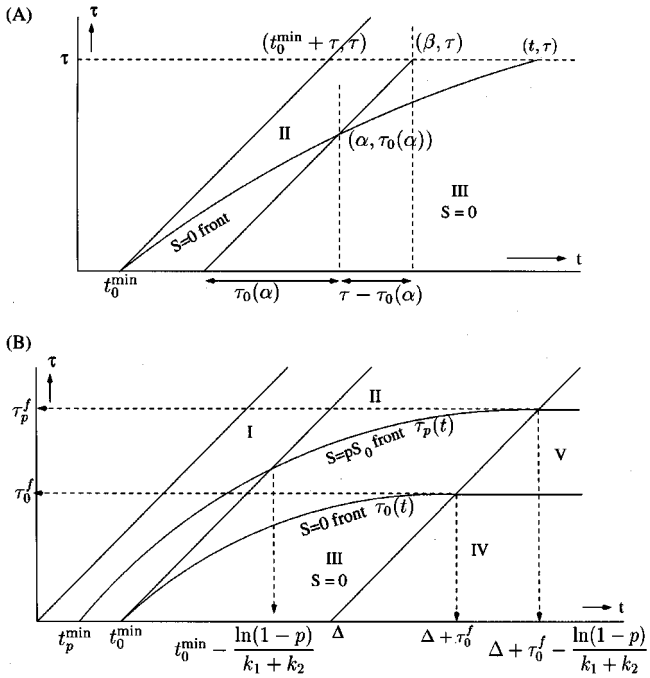

Figure 2. (A) Dithionite waves originating in region III overtake the $S = 0$ front to enter region II; (B) propagation of $S = pS_0$ front when $\Delta > t_0^{\min}$.

Referring to (A), their intersection point determines the time duration, the two reaction models (Eqs. 3 and 4 apply along the characteristic).

this τ during this time interval intersect the $S = 0$ front. Consider a characteristic passing through (β,τ) and intersecting the $S = 0$ front at $[\alpha, \tau_0(\alpha)]$, as shown in Figure 2A. Clearly, as β goes from $t_0^{\min} + \tau$ to t, α goes from $t_0^{\min}$ to t. Because dithionite reacts according to Eq. 4 in region III and, according to Eq. 3, in region II we can evaluate C and S at (β,τ)

$$\beta = \alpha + \tau - \tau_0(\alpha) \tag{11}$$

$$\begin{aligned} C(\beta,\tau) &= C_i \exp\left[-k_2\tau_0(\alpha)\right]\exp\left[-(k_1+k_2)(\tau-\tau_0(\alpha))\right] \\ &= C_i \exp\left[-(k_1+k_2)\tau\right]\exp\left[k_1\tau_0(\alpha)\right] \end{aligned} \tag{12}$$

$$\begin{aligned} S(\beta,\tau) &= S_0 - 2k_1\int_0^{\beta} C(\beta,\tau)\,d\beta = S\left(t_0^{\min}+\tau,\tau\right) \\ &\quad - 2k_1\int_{t_0^{\min}+\tau}^{\beta} C(\beta,\tau)\,d\beta \\ &= S_0 - 2k_1C_i\exp\left[-(k_1+k_2)\tau\right] \\ &\quad \times\left[t_0^{\min} + \int_{t_0^{\min}+\tau}^{\beta}\exp\left[k_1\tau_0(\alpha)\right]d\beta\right] \end{aligned} \tag{13}$$

Because τ will become a part of region III when $\tau = \tau_0(t)$

$$\begin{aligned} 0 &= S_0 - 2k_1C_i\exp\left[-(k_1+k_2)\tau_0(t)\right] \\ &\quad \times\left[t_0^{\min} + \int_{t_0^{\min}}^{t}\exp\left[k_1\tau_0(\alpha)\right]\left[1-\dot{\tau}_0(\alpha)\right]d\alpha\right] \end{aligned} \tag{14}$$

Differentiation with respect to t yields $d\tau_0/dt = 1/[1 + t_0^{\min}(k_1 + k_2)\exp(k_2\tau_0)]$. Upon integration from $[t_0^{\min},0]$ to $[t,\tau_0(t)]$

$$t = t_0^{\min}\left[1 + \frac{k_1 + k_2}{k_2}\left[\exp(k_2\tau_0) - 1\right]\right] + \tau_0 \qquad (15)$$

which is the equation for the propagation of the $S = 0$ front, $\tau_0(t)$.

Solution in Region II. With the location of the $S = 0$ front known, its intersection with any characteristic passing through a location (t,τ) in region II can be evaluated. Using the abscissa of the intersection in Eqs. 12 and 13, we get for region II

$$C(t,\tau) = C_i \exp\left[-(k_1 + k_2)\tau\right]\left[\frac{k_2(t-\tau) + k_1 t_0^{\min}}{(k_1 + k_2)t_0^{\min}}\right]^{k_1/k_2} \qquad (16)$$

$$S(t,\tau) = S_0 - 2k_1 C_i t_0^{\min}\exp\left[-(k_1 + k_2)\tau\right] \times \left[\frac{k_2(t-\tau) + k_1 t_0^{\min}}{(k_1 + k_2)t_0^{\min}}\right]^{(k_1 + k_2)/k_2} \qquad (17)$$

It is easy to show that when $\tau = \tau_0(t)$, Eqs. 16 and 17 reduce to Eq. 10; and when $\tau = t - t_0^{\min}$, they reduce to Eqs. 6 and 7. Thus, C and S remain continuous across the boundaries between regions II and III and regions II and I.

Regions IV and V

For time $t > \Delta$, the injection continues but without dithionite. As shown in Figure 1B, the trailing edge of the dithionite pulse propagates along the unit-slope characteristic originating at $(t = \Delta, \tau = 0)$. The $t - \tau$ region to its right is dithionite free, so S will not change with time in regions IV and V. The trailing edge of the dithionite pulse intersects and overtakes the slower-moving $S = 0$ front at time $\Delta + \tau_0^f$. Once this occurs, the position of the $S = 0$ front cannot advance because there is no dithionite at the front. τ_0^f is the final value for $\tau_0(t)$. Regions IV and V are separated by the line $\tau = \tau_0^f$. τ_0^f is determined from Eq. 15 as $\tau_0(\Delta + \tau_0^f)$.

$$\tau_0^f = \frac{1}{k_2}\ln\left[\frac{k_2\Delta + k_1 t_0^{\min}}{(k_1 + k_2)t_0^{\min}}\right] = \frac{1}{k_2}\ln\left[\frac{k_1(2k_2 C_i\Delta + S_0)}{(k_1 + k_2)S_0}\right] \qquad (18)$$

An important result here is that the final width of the $S = 0$ zone is a function only of the product $C_i\Delta$ (which is proportional to the total amount of dithionite injected), and not of C_i and Δ individually. So, for a given mass of dithionite, τ_0^f can be achieved quickly by using a large value for C_i (implying a shorter pulse length Δ), because the time at which $\tau_0(t) = \tau_0^f$ is $\Delta + \tau_0^f$. Region V is dithionite free, with S as nonzero. A position τ in region II would become a part of region V at time $t = \Delta + \tau$ when the trailing edge of the dithionite pulse arrives at that τ. So, the constant value for S at that τ is equal to $S(\Delta + \tau,\tau)$, as given by Eq. 17 when that τ was a part of region II. This is given by

$$S(t,\tau) = S_0 - 2k_1 C_i t_0^{\min}\exp\left(-(k_1 + k_2)\tau\right) \times \left[\frac{k_2\Delta + k_1 t_0^{\min}}{(k_1 + k_2)t_0^{\min}}\right]^{(k_1 + k_2)/k_2}. \qquad (19)$$

Propagation of $S = pS_0$ front

Now formulae are developed for the propagation of the reduction zone that needs to be maximized in a field design. The propagation of the front $S = pS_0$ for $0 < p < 1$ is considered. The propagation of $S = 0$ front ($p = 0$), $\tau_0(t)$ has already been derived as part of the solution in Eq. 15, and the position of $S = S_0$ front ($p = 1$), $\tau_1(t)$ is simply equal to t. Using $S(t = t_p^{\min}, \tau = 0) = pS_0$, the minimum time for the formation of the $\tau_p(t)$ front is obtained from Eq. 7

$$t_p^{\min} = (1 - p)t_0^{\min} \qquad (20)$$

If the duration Δ of the pulse is less than $t_p^{\min}$, S will not decrease to pS_0 anywhere. If $t_0^{\min} > \Delta > t_p^{\min}$, the τ_p front forms in region I in Figure 1A and attains its final position, τ_p^f, at time $\Delta + \tau_p^f$ when it moves into region I′. The propagation of the τ_p front during this time is obtained by applying Eq. 7. Using $S(t = \Delta + \tau_p^f, \tau = \tau_p^f) = pS_0$ in Eq. 7, and solving for the final position, τ_p^f

$$\tau_p^f = \frac{1}{k_1 + k_2}\ln\left[\frac{\Delta}{t_p^{\min}}\right] \qquad (21)$$

Figure 2B shows the propagation of the τ_p front when $\Delta > t_0^{\min}$. The τ_p front is in region I during the time interval $t_p^{\min} \le t \le t_0^{\min} - [\ln(1 - p)]/(k_1 + k_2)$. For $\Delta + \tau_p^f > t > t_0^{\min} - [\ln(1 - p)]/(k_1 + k_2)$, the τ_p front is in region II. The trailing edge of the dithionite pulse overtakes τ_p front at time $\Delta + \tau_p^f$, after which the τ_p front stops expanding. τ_p^f is the final position of the τ_p front. Equation 17 applies when the τ_p front is in region II so that τ_p^f is obtained by solving $S(t = \Delta + \tau_p^f, \tau = \tau_p^f) = pS_0$ for τ_p^f

$$\tau_p^f = -\frac{\ln(1 - p)}{k_1 + k_2} + \frac{1}{k_2}\ln\left[\frac{k_2\Delta + k_1 t_0^{\min}}{(k_1 + k_2)t_0^{\min}}\right] = -\frac{\ln(1 - p)}{k_1 + k_2} + \tau_0^f \qquad (22)$$

Optimal Delivery of Dithionite

Having the complete solution in hand, operational parameters such as well flow rates, number of wells and their configurations, injection concentration C_i, and the pulse length Δ needed to establish a barrier of certain shape and dimensions are selected. Legitimate objectives for the design include minimizing the amount of dithionite or the total cost per unit

area of barrier. While injection/extraction wells are the means to establish a flow pattern and deliver dithionite in the field, numerous configurations with different time-varying flow rates and injection concentrations are possible; thus, there are a large number of variables that may be considered as vehicles for achieving an optimal design. Further, constraints such as a fixed number of wells and/or total time of operation are also conceivable. Despite the availability of an analytic solution, a simultaneous consideration of all the options and constraints would lead to a complex multivariable, multiconstraint, mixed-integer optimization problem, which is beyond the scope of this article. Instead, a simpler problem is solved by using: (a) time-invariant flow rate Q; (b) constant injection concentration C_i for the duration $0 \le t \le \Delta$; (c) a single injection well to deliver dithionite. Also, because $C_i\Delta = M/Q$, where M is the amount of dithionite injected, the final position of the τ_p front (Eqs. 21 and 22) can be conveniently expressed as

$$\tau_p^f = 0 \qquad \text{if} \quad Q > \frac{yz}{(1-y)(1-p)} \tag{23}$$

$$\tau_p^f = \frac{1}{k_1+k_2}\ln\left[\frac{y}{(1-y)(1-p)}\frac{z}{Q}\right] \qquad \text{if} \quad \frac{yz}{(1-y)(1-p)} > Q > \frac{yz}{1-y} \tag{24}$$

$$\tau_p^f = \frac{1}{k_2}\ln\left[\frac{y\left(1+\frac{z}{Q}\right)}{(1-p)^{(1-y)}}\right] \qquad \text{if} \quad Q < \frac{yz}{1-y} \tag{25}$$

where

$$z = 2k_2 M/S_0 \quad \text{and} \quad y = k_1/(k_1+k_2) \tag{26}$$

Because the reduction zone is known in terms of the injection rate Q, and total available mass M of dithionite, Q can be considered as the variable to optimize on and M as the constraint. We can now state our simpler optimization problem as the following:

Given the total available mass M of dithionite, find the optimal injection rate Q that maximizes the $S \le pS_0$ region for some p, $0 \le p < 1$.

A series of such optimally operating injection wells can then be used to build the redox barrier of the required shape and dimensions. The aquifer is confined and homogeneous, and the well fully penetrating, so that a radial flow field is established. Without loss of generality, porosity ϕ is taken to be unity because its effect is simply to reduce the travel-time to any radial distance r by the factor ϕ. The complete solution to the radial propagation of dithionite is obtained by transforming the τ-axis in Figure 1 according to the relationship between $\tau(r)$ and r in a radial flow field. The travel-time $\tau(r)$ (days) from the injection well to any distance r (meters) in a radial flow field set up by an injection rate of Q (m^3/day) in an aquifer of depth H (meters) is given by

$$\tau(r) = H\pi r^2/Q, \quad \text{or} \quad r = \sqrt{Q/(H\pi)}\sqrt{\tau(r)} \tag{27}$$

Equation 27 neglects the natural aquifer flow that should be superposed on the forced radial flow established by injection. This is fine near the injection, where radial flow dominates, but is erroneous far from the injection well where the ambient flow is expected to dominate. But, given the relatively fast consumption rates for dithionite, the radial distance over which a significant reduction of Fe(III) can be achieved is usually well short of the distance at which the speed of ambient flow becomes comparable to that of forced flow. So, the analysis presented in this section is not adversely affected by neglecting the ambient flow field. Those situations characterized by fast groundwater flow, slow reaction rates, small Q, and a large value for p warrant the consideration of a combined flow field. Had a completely different mechanism such as a dipole (an injection-extraction pair of wells) been considered for delivering dithionite, then also the flow field would be different. Whatever the reason might be for the different flow field, Eq. 27 is simply replaced with a different, appropriate equation that relates the field location to the travel-time τ along a streamline originating at the injection location. While the algebra becomes more involved (there will not be a radial symmetry), the methodology in all these cases remains identical to what is presented here.

Using Eq. 27, in Eqs. 23 through 25, the final position of the r_p^f front in this radial flow field is obtained as

$$r_p^f\sqrt{k_2/z} = 0 \qquad \text{if} \quad \frac{Q}{z} > \frac{y}{(1-y)(1-p)} \tag{28}$$

$$r_p^f\sqrt{k_2/z} = \sqrt{\frac{Q(1-y)}{H\pi z}}\left[\ln\left(\frac{y}{(1-y)(1-p)}\frac{z}{Q}\right)\right]^{1/2} \qquad \text{if} \quad \frac{y}{(1-y)(1-p)} > \frac{Q}{z} > \frac{y}{1-y} \tag{29}$$

$$r_p^f\sqrt{k_2/z} = \sqrt{\frac{Q}{H\pi z}}\left[\ln\left(\frac{y(1+z/Q)}{(1-p)^{(1-y)}}\right)\right]^{1/2} \qquad \text{if} \quad \frac{Q}{z} < \frac{y}{1-y} \tag{30}$$

An interesting conclusion from Eqs. 29 and 30 is that, when M/Q is a constant, the area of $S \le pS_0$ zone is simply proportional to Q. So the area of $S \le pS_0$ zone established by a single injection well with a given M and Q will be the same as the total area of $S \le pS_0$ zones established by n injection wells, each operating with M/n as the dithionite mass and Q/n as the flow rate.

Example

For illustration, consider an injection well operating with $Q = 17.88$ m^3/day (≈ 3.3 gal/min), and $M = 3{,}576$ moles in an aquifer of depth $H = 1.0$ m. Figure 3 shows the propagation of C, S profiles when the injection concentration C_i of dithionite is 0.1 mol/L and $\Delta \equiv M/(QC_i)$ is 2.0 days. The solution is obtained by first computing $C(t,\tau)$ and $S(t,\tau)$ according to Figure 1 and then using Eq. 27 to express it in

terms of (t,r). The minimum duration $t_0^{\min}$ of the dithionite pulse needed to establish $S=0$ zone is obtained from Eq. 8 as 0.125 days. Because the pulse employed here is longer, the solution exhibits the behavior shown in regions I through V in Figure 1B. When $t=0.625$ days, which is greater than $t_0^{\min}$ but less than Δ, the solution exhibits regions III, II, and I as r goes from 0 to 1.886 m. The position of the Fe(III)-free zone is extended up to $r_0(t)\approx 1.4$ m. When $t=2.5$ days, the solution displays regions IV, III, II, and I, as r goes from 0 to 3.772 m with $r_0(t)\approx 2.746$ m. The travel-time τ_0^f is 1.792 days, so at time $t=\Delta+\tau_0^f=3.792$ days, region IV overtakes and eliminates region III. At this time, $r_0(t)$ assumes its final position r_p^f approximately equal to 3.19 m. When $t=4.0$ days, the solution exhibits regions IV, V, II, and I as r goes from 0 to 4.771 m, with the profile for $S[r_0^f(\approx 3.19\text{ m}) \le r \le \sqrt{Q(t-\Delta)/(H\pi)}\,(\approx 3.37\text{ m})]$ unchanging for all future times. So when $t=5.0$ days, the profile for S differs from that at $t=4.0$ days only for $r>3.37$ m.

Optimal injection rate

Optimal Q is the injection rate at which r_p^f is maximized for a given mass M of dithionite injected at the well. It is clear from Eqs. 24 and 25 that τ_p^f decreases as Q increases so the maximum τ_p^f is obtained by using a small Q. But, r_p^f is maximized when $Q\tau_p^f$ is maximized, so the maximum of r_p^f may be obtained for small Q and large τ_p^f (Eq. 30) or vice versa (Eq. 29). Figure 4 illustrates the behavior of Eqs. 29 and 30 for two values of p, 0.25 and 0.75, when $y=0.5$. When the required reduction is greater ($p=0.25$), a larger r_p^f is obtained by using a smaller Q that allows the formation of the $S=0$ front. On the contrary, when the required reduction is smaller ($p=0.75$), a larger r_p^f is obtained by using a larger Q that does not allow the formation of $S=0$ front. This observation is rigorously quantified in the following.

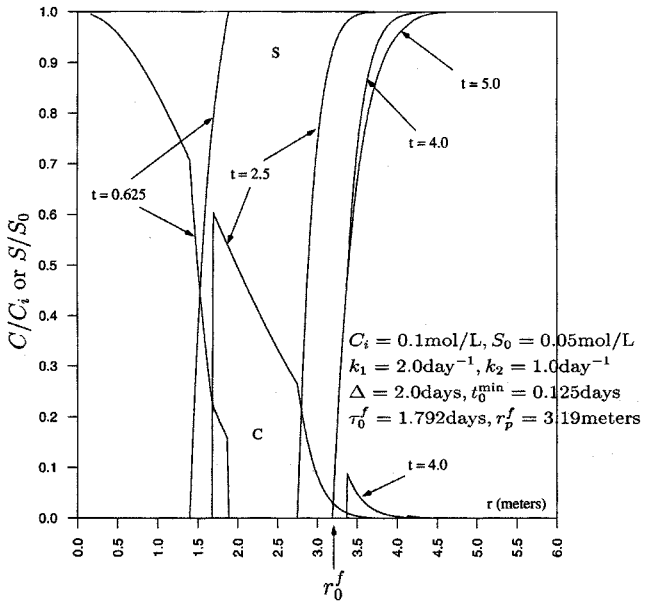

Figure 3. Propagation of C, S profiles and the formation of reduction zone in a radial flow field with $Q=17.88$ m^3/day, $M\equiv QC_i\Delta=3{,}576$ mol/d.

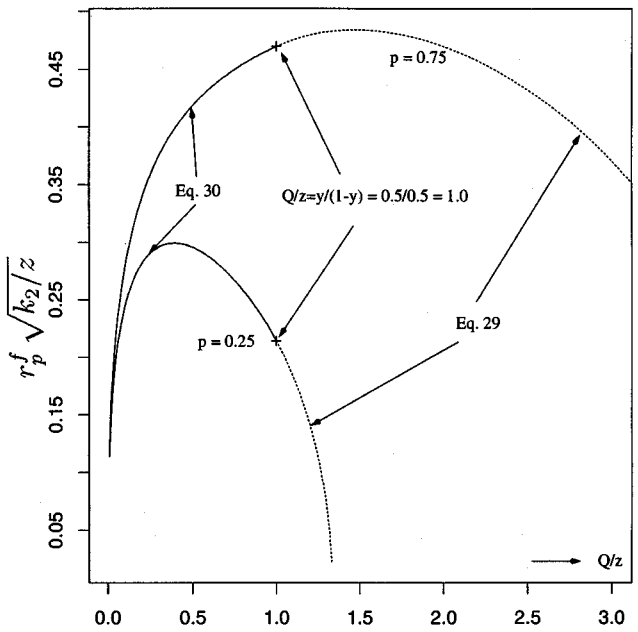

Figure 4. Allowing the formation of $S=0$ front by requiring $Q<yz/(1-y)$ yields a larger r_p^f when $0\le p\le 1-\exp(-1.0)$.

Not allowing its formation by requiring $yz/[(1-y)(1-p)]>Q>yz/(1-y)$ yields a larger r_p^f when $1-\exp(-1.0)\le p<1$.

For a given amount of dithionite, a fast injection rate does not allow sufficient residence time to create an Fe(II) zone of sufficient concentration, whereas a slower injection rate allows excessive loss of dithionite through disproportionation. So, there exists an optimal injection rate that maximizes the size of Fe(III) reduced zone for a given mass of dithionite. First, consider Eq. 29, which applies when $yz/(1-y)(1-p)\ge Q\ge yz/(1-y)$. $r_p^f(Q)$ is strictly convex, but $dr_p^f/dQ=0$ has a solution only for $p>1-\exp(-1.0)$.

$$Q_p^{\text{opt}}/z=\frac{y\exp(-1.0)}{(1-y)(1-p)},\quad r_p^{\max}\sqrt{k_2/z}=\left[\frac{y\exp(-1.0)}{H\pi(1-p)}\right]^{1/2}\qquad p>1-\exp(-1.0)\quad(31)$$

Second, when $Q<yz/(1-y)$, $r_p^f(Q)$ (Eq. 30) is once again strictly convex, but $dr_p^f/dQ=0$ has a solution only for $p<1-\exp(-1.0)$. Solving $dr_p^f/dQ=0$ for Q_p^{opt},

$$Q_p^{\text{opt}}/z=-\frac{W\left[-y(1-p)^{(y-1)}\exp(-1.0)\right]}{1+W\left[-y(1-p)^{(y-1)}\exp(-1.0)\right]},\qquad p<1-\exp(-1.0)\quad(32)$$

where W is the Lambert W function (Corless et al., 1993, 1996). Note that W should be evaluated on its principal branch. This is because $y(1-p)^{(y-1)}<1.0$ for $p<1-$

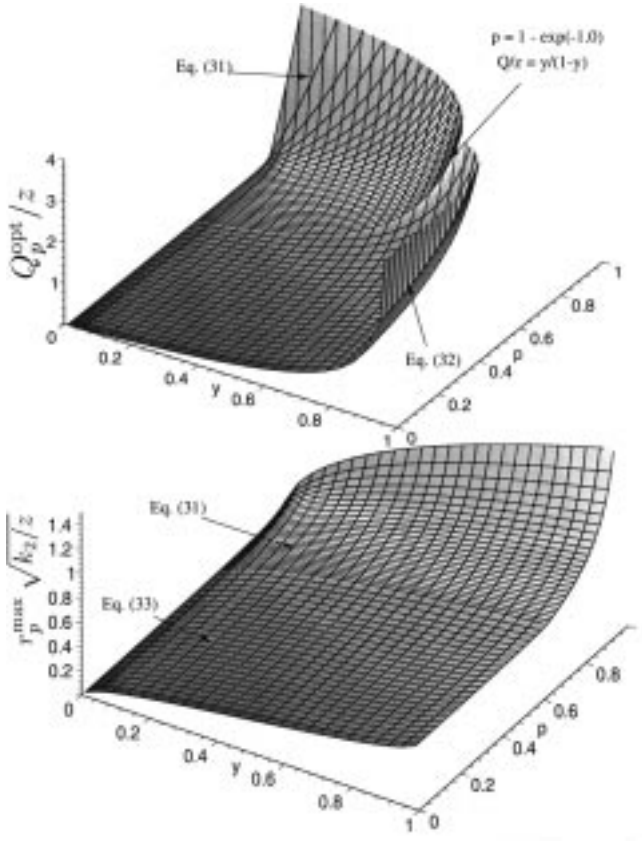

Figure 5. Surfaces Q_p^{opt}/z and $r_p^{max}\sqrt{k_2/z}$ made up of two sheets that join at $p = 1 - \exp(-1.0)$, along which $Q_p^{opt}/z = y/(1-y)$ and $r_p^{max}\sqrt{k_2/z} = [y/(H\pi)]^{0.5}$.

$\exp(-1.0)$, and only the principal branch value of $W[-y(1-p)^{(y-1)}\exp(-1.0)]$ lies between 0 and -1, thus guaranteeing a positive value for Q_p^{opt}/z. Using this in Eq. 30,

$$r_p^{max}\sqrt{k_2/z} = \sqrt{\frac{1}{H\pi}}\left[-\frac{W\left[-y(1-p)^{(y-1)}\exp(-1.0)\right]}{1+W\left[-y(1-p)^{(y-1)}\exp(-1.0)\right]}\right]^{1/2}\left[\ln\left[\frac{-y(1-p)^{(y-1)}}{W\left[-y(1-p)^{(y-1)}\exp(-1.0)\right]}\right]\right]^{1/2} \quad (33)$$

Figure 5 shows the optimal surface of Q_p^{opt}/z and the surface of maximum $r_p^{max}\sqrt{k_2/z}$ as a function of p and y.

The well should be operated for a minimum period of $\Delta + \tau_p^f = \Delta + H\pi(r_p^{max})^2/Q_p^{opt}$ at which time r_p^{max} is established. If Q_p^{opt} is too large to be practical, then a series of n injection wells, each with an injection rate of Q_p^{opt}/n and an injection mass of M/n of dithionite, can be used because we know that the total reduction zone (with $S \le pS_0$) area obtained would be the same. When multiple injection wells are needed, a small improvement to this total area can be achieved by allowing a partially reduced (less than the desired reduction) zone created by one well to overlap the similar zone created by the adjacent well, thereby achieving the required reduction to $S = pS_0$.

To Sum Up

The potential of *in situ* reduction zones in remediating contaminated groundwater by removing redox sensitive contaminants such as chromium, uranium, and some chlorinated compounds has elicited much interest. This article has studied the reduction of subsurface Fe(III) oxides to create a reducing Fe(II) zone by injecting a sodium dithionite solution. The model for the interaction of dithionite with Hanford sediments consists of a redox reaction that generates Fe(II) out of Fe(III), and a disproportionation reaction that results in a waste of dithionite. The main feature of the solution to this problem is the development and propagation of a Fe(III)-free zone, in which a different reaction model applies.

The flow field due to a single injection well is studied for its ability to deliver dithionite and create a reduced barrier. The reduction zone created by a single injection well with a large rate Q and mass M is identical to the total area of reduced zones created by n injection wells, each operating with a rate Q/n and using a mass M/n. The optimal injection rate that maximizes the radius of the reduction zone where $S \le pS_0 (p < 1)$ is proportional to $k_2 M/S_0$, with the constant of proportionality being a function only of the ratio $k_1/(k_1 + k_2)$ and p. k_1 and k_2 are the rate constants for the redox and disproportionation reactions, respectively. When $p \le 1 - \exp(-1.0)$, it is better to allow the formation of the Fe(III)-free zone, whereas for $p \ge 1 - \exp(-1.0)$, not allowing its formation will yield a larger reduction zone. The maximum radius obtained is proportional to $\sqrt{M/S_0}$, where once again the constant of proportionality is a function only of the ratio $k_1/(k_1 + k_2)$ and p.

Acknowledgments

The author is indebted to an anonymous reviewer for a number of valuable suggestions that have improved this article. The author is also grateful to Mark D. Williams, whose comments were very helpful in the development of this article. Pacific Northwest National Laboratory is operated for the U.S. Dept. of Energy (DOE) by Battelle Memorial Institute, under Contract DE-AC06-76RLO 1830.

Literature Cited

Amonette, J., J. Szecsody, H. Schaef, J. Templeton, Y. Gorby, and J. Fruchter, "Abiotic Reduction of Aquifer Materials by Dithionite: A Promising in-situ Remediation Technology," *In-Situ Remediation: Scientific Basis for Current and Future Technologies*, G. Gee and N. Wing, eds., p. 851, Battelle Press, Columbus, OH (1994).

Anderson, L., D. Kent, and J. Davis, "Batch Experiments Characterizing the Reduction of Cr(VI) Using Suboxic Material from a Mildly Reducing, Sand and Gravel Aquifer," *Env. Sci. and Technol.*, **28**, 174 (1994).

Chilakapati, A., and S. Yabusaki, "Nonlinear Reactions and Nonuniform Flows," *Water Resour. Res.*, in press (1999).

Corless, R., G. Gonnet, D. Hare, and D. Jeffrey, "On the Lambert's W Function, Tech. Rep," Technical report CS-93-03, University of Waterloo, Canada (1993).

Corless, R., G. Gonnet, D. Hare, D. Jeffrey, and D. Knuth, "A Sequence of Series for the Lambert W Function," *Adv. in Comp. Math.*, **5**, 329 (1996).

Cvetkovic, V., and G. Dagan, "Transport of Kinetically Sorbing

Solute by Steady Random Velocity in Heterogeneous Porous Formations,'' *J. of Fluid Mechanics*, **265**, 189 (1994).
Friedly, J., J. Davis, and D. Kent, ''Modeling Hexavalent Chromium Reduction in Groundwater in Field-Scale Transport and Laboratory Batch Experiments,'' *Water Resour. Res.*, **31**, 2783 (1995).
Fruchter, J., et al., ''In-Situ Redox Manipulation Field Injection Test Report—Hanford 100-H Area,'' Technical Report 11372, Pacific Northwest National Laboratory (1996).
Gorby, Y., J. Amonette, and J. Fruchter, ''Remediation of Contaminated Subsurface Materials by a Metal-Reducing Bacterium,'' *In-Situ Remediation: Scientific Basis for Current and Future Technologies*, G. Gee and N. Wing, eds., Battelle Press, Columbus, OH, p. 234 (1994).
Istok, J., et al., ''In Situ Redox Manipulation by Dithionite Injection: Intermediate-Scale Laboratory Experiments,'' *Groundwater*, submitted (1999).
Kent, D., J. Davis, L. Anderson, and B. Rea, ''Transport of Chromium and Selenium in the Suboxic Zone of a Shallow Aquifer: Influence of Redox and Adsorption Reactions,'' *Water Resour. Res.*, **30**, 1099 (1994).
Lovely, D., ''Dissimilatory Metal Reduction,'' *Ann. Rev. Microbiol.*, **47**, 263 (1993).
Reidel, S., N. Campbell, K. Fecht, and K. Lindsey, ''Late Cenozoic Structure and Stratigraphy of South-Central Washington,'' *Regional Geology of Washington State*, Washington Div. of Geology and Earth Resources, p. 159 (1994).
Sass, B., and D. Rai, ''Solubility of Amorphous Chromium(iii)-Iron(iii) Hydroxide Solid Solutions,'' *Inorganic Chemistry*, **26**, 2228 (1987).
Szecsody, J. E., A. Chilakapati, J. Zachara, and A. Garvin, ''Influence of Iron Oxide Inclusion Shape on Co(II/III)EDTA Reactive Transport through Spatially Heterogeneous Sediment,'' *Water Resour. Res.*, **34**, 2501 (1998).
Williams, M., S. Yabusaki, C. Cole, and V. Vermeul, ''In-Situ Redox Manipulation Field Experiment: Design Analysis,'' *In-Situ Remediation: Scientific Basis for Current and Future Technologies*, G. Gee and N. Wing, eds., Battelle Press, Columbus, OH (1994).

Manuscript received Sept. 3, 1998, and revision received Mar. 17, 1999.